J. Fluid Mech. (1994), *vol.* 259, *pp.* 333–344

Crest instabilities of gravity waves. Part 2. Matching and asymptotic analysis

By MICHAEL S. LONGUET-HIGGINS[1], R. P. CLEAVER[2] AND M. J. H. FOX[3]

[1] Institute for Nonlinear Science, University of California, San Diego, La Jolla, CA 92093-0402, USA

[2] Gas Research Centre, British Gas, Ashby Road, Loughborough LE11 3QU, UK

[3] Berkeley Nuclear Laboratories, Nuclear Electricity plc, Berkeley, Gloucestershire GL13 9PB, UK

(Received 11 June 1993 and in revised form 16 September 1993)

In a previous study (Longuet-Higgins & Cleaver 1994) we calculated the stability of the flow near the crest of a steep, irrotational wave, the 'almost-highest' wave, considered as an isolated wave crest. In the present paper we consider the modification of this inner flow when it is matched to the flow in the rest of the wave, and obtain the normal-mode perturbations of the modified inner flow. It is found that there is just one exponentially growing mode. Its rate of growth β is a decreasing function of the matching parameter ϵ and hence a decreasing function of the wave steepness ak. When compared numerically to the rates of growth of the lowest superharmonic instability in a deep-water wave as calculated by Tanaka (1983) it is found that the present theory provides a satisfactory asymptote to the previously calculated values of the growth rate. This suggests that the instability of the lowest superharmonic is essentially due to the flow near the crest of the wave.

1. Introduction

The present paper is a sequel to a recent investigation (Longuet-Higgins & Cleaver 1994, referred to herein as LHC) in which the problem of wave breaking was tackled by considering the stability of the flow in an 'almost-highest wave', that is to say the asymptotic form assumed by the crest of a steep, irrotational gravity wave as the limiting Stokes corner flow is approached, but while the crest is still rounded (see Longuet-Higgins & Fox 1977, referred to herein as LHF1). It was found that there exists just one unstable normal-mode perturbation of this flow, with a form resembling the initial stages of a spilling breaker.

The question then arises: how is this local instability of a gravity wave crest related to the known unstable modes of perturbation of a progressive gravity wave? For example, it was shown numerically by Tanaka (1983) and Longuet-Higgins (1986) and analytically by Saffman (1985), that the lowest superharmonic perturbation becomes unstable at a value of the wave steepness parameter $ak = 0.4292$, corresponding to the first maximum in the wave energy density as a function of ak. Is this superharmonic instability essentially the result of the local flow near the wave crest?

Now the 'almost-highest wave' considered in LHF1 and LHC is the inner flow near the wave crest, in terms of a small parameter ϵ which measures departure of the flow from an ideal Stokes corner flow. Thus we may define

$$\epsilon = q_0/2c, \tag{1.1}$$

where q_0 is the particle speed at the crest, in a frame moving horizontally with the wave-speed c. For small values of ϵ the flow near the crest (within a distance of order ϵ^2) is described by the 'almost-highest' wave. However, if we wish to calculate the properties of progressive waves with slightly less than the limiting steepness, this inner flow must be matched asymptotically to the 'outer flow' in the rest of the wave, as described by Longuet-Higgins & Fox (1978, referred herein to as LHF2). It was there shown that this approach of working downwards from the wave of limiting steepness predicts successfully the surface profile, the wave speed, and other integral properties as a function of the steepness ak.

The process of matching the inner and outer flows introduces a small correction to the inner flow, of order $\epsilon^{3(\lambda-1)}$, where λ is the root of a transcendental equation; see LHF2. Our hypothesis is that the perturbations of the corrected inner flow will yield the asymptotic behaviour of the superharmonic instability, and hence show that it is essentially an instability of the flow in the wave crest.

An outline of the paper is as follows. In §2 we describe the matching technique and in §§3 and 4 determine the corrected inner flow, as in Fox (1977). In §5 we derive equations for the perturbation of this inner flow. In fact these are given by a modification to the correcting equations for the original inner flow, as derived in LHC. The results of the calculations are described and discussed in §6.

2. The matching technique

We shall use the same notation and coordinates as in LHC, choosing units of mass, length and time so that the fluid density and the gravitational acceleration g are both unity. The wavelength is taken to be 2π.

As was seen in §2 of LHF2, the fluid domain in any steep, progressive wave may be divided into three distinct zones: an inner zone I of radius ϵ^2 centred on the wave crest, in which typical lengths are of order ϵ^2 and typical velocities are $O(\epsilon)$; an intermediate zone II, where typical lengths and velocities are of order ϵ and $\epsilon^{\frac{1}{2}}$ respectively; and an outer zone III where lengths and velocities are of order unity; see figure 1. Thus in Zone I we have

$$z = \epsilon^2 z_1, \quad \chi = \epsilon^3 \chi_1, \tag{2.1}$$

where z_1 and χ_1 are of order unity. From LHF1 we know that

$$z_1 = (\tfrac{3}{2}\mathrm{i}\chi_1)^{\frac{2}{3}}(1+R), \tag{2.2}$$

where

$$R = C(\mathrm{i}\chi_1)^{-(1+\mathrm{i}\mu)} + C^*(-\mathrm{i}\chi_1)^{-(1-\mathrm{i}\mu)}, \tag{2.3}$$

C is a constant and μ is the positive root of

$$\frac{\pi\mu}{2}\tanh\frac{\pi\mu}{2} = \frac{\pi}{2\sqrt{2}}, \tag{2.4}$$

viz. $\mu = 0.7143\ldots$. As $\chi_1 \to \infty$, so clearly $R \to 0$ and

$$z_1 \sim (\tfrac{3}{2}\mathrm{i}\chi)^{\frac{2}{3}}, \tag{2.5}$$

representing the Stokes 120° corner-flow.

On the other hand in Zone III we know from LHF2 (see also Grant 1973) that in the limit $\epsilon \to 0$ (a sharp-crested, limiting wave), and as $\chi \to 0$ (the neighbourhood of the sharp crest), so

$$z \sim (\tfrac{3}{2}\mathrm{i}\chi)^{\frac{2}{3}}[1 + \gamma(\mathrm{i}\chi)^{\lambda-1}], \tag{2.6}$$

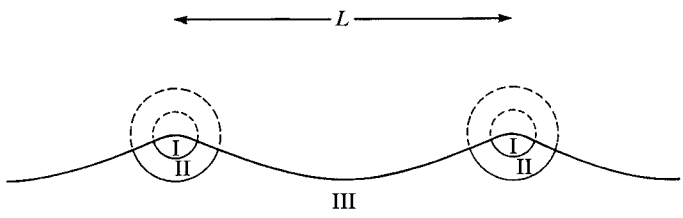

FIGURE 1. (after LHF2). Sketch showing regions of validity for the inner solution (Zone I), outer solution (Zone III) and matching of the two solutions (Zone II).

where λ is the lowest positive root of

$$\frac{\pi\lambda}{2}\tan\frac{\pi\lambda}{2} = -\frac{\pi}{2\sqrt{3}}, \tag{2.7}$$

namely

$$\lambda = 1.8027\ldots \tag{2.8}$$

and γ is a constant. It was found numerically in LHF2, §3, that for a progressive wave on deep water

$$(\tfrac{3}{2})^{\frac{2}{3}}\gamma = 0.131 \quad \text{so} \quad \gamma = 0.100. \tag{2.9}$$

Now by matching the solutions in Zone II, as in §2 of LHF2, we see that the inner flow (2.2) has to be modified as in equation (2.6), that is by multiplying by a factor F such that when $\chi_1 \to \infty$

$$\begin{aligned} F &\sim 1+\gamma(\mathrm{i}\chi)^{\lambda-1} \\ &= 1+\gamma(\mathrm{i}\epsilon^3\chi_1)^{\lambda-1} \\ &= 1+\gamma\eta(\mathrm{i}\chi_1)^{\lambda-1}, \end{aligned} \tag{2.10}$$

where

$$\eta = \epsilon^{3(\lambda-1)} = \epsilon^{2.481}. \tag{2.11}$$

This defines the behaviour of the inner flow for large values of χ_1.

3. Determination of the inner flow

To derive complete equations for the inner flow we introduce as in LHF1 the transformation

$$\frac{\delta-\mathrm{i}\chi_1}{\delta+\mathrm{i}\chi_1} = \omega, \quad |\omega| \leqslant 1 \tag{3.1}$$

and write

$$z_1 = (\delta+\mathrm{i}\chi_1)^{\frac{2}{3}}B(\omega)+\eta(\delta+\mathrm{i}\chi_1)^{\lambda-\frac{1}{3}}\tilde{B}(\omega), \tag{3.2}$$

where

$$B(\omega) = B_0+B_1\omega+B_2\omega^2+\ldots \tag{3.3}$$

as before, and

$$\tilde{B}(\omega) = \tilde{B}_0+\tilde{B}_1\omega+\tilde{B}_2\omega^2+\ldots. \tag{3.4}$$

By equation (2.10) we have that as $\chi_1 \to \infty$ so

$$\begin{aligned} z_1 &\sim (\delta+\mathrm{i}\chi_1)^{\frac{2}{3}}B(\omega)[1+\gamma\eta(\mathrm{i}\chi_1)^{\lambda-1}] \\ &\sim (\delta+\mathrm{i}\chi_1)^{\frac{2}{3}}B(\omega)[1+\gamma\eta(\delta+\mathrm{i}\chi_1)^{\lambda-1}] \\ &= (\delta+\mathrm{i}\chi_1)^{\frac{2}{3}}B(\omega)+\gamma\eta(\delta+\mathrm{i}\chi_1)^{\lambda-\frac{1}{3}}B(\omega). \end{aligned} \tag{3.5}$$

Comparing (3.2) and (3.5) we see that

$$\tilde{B}(\omega) \sim \gamma B(\omega) \quad \text{as} \quad \chi_1 \to \infty, \tag{3.6}$$

that is, as $\omega \to -1$. Hence

$$\tilde{B}(-1) = \gamma B(-1). \tag{3.7}$$

But from (2.2) and (3.2) we have

$$B(-1) = (\tfrac{3}{2})^{\frac{2}{3}} = 1.3104. \tag{3.8}$$

Thus we must have

$$\tilde{B}_0 - \tilde{B}_1 + \tilde{B}_2 + \ldots = \tilde{B}(-1) = 0.100. \tag{3.9}$$

We specify also that $\tilde{B}(\omega)$ vanishes at the wave crest ($\omega = 1$), and so

$$\tilde{B}_0 + \tilde{B}_1 + \tilde{B}_2 + \ldots = \tilde{B}(1) = 0. \tag{3.10}$$

4. The free-surface condition for $\tilde{B}(\omega)$

The condition of constant pressure at the free surface may be written

$$(z + z^*)\frac{\mathrm{d}z}{\mathrm{d}\chi}\frac{\mathrm{d}z^*}{\mathrm{d}\chi^*} = 1 \tag{4.1}$$

(see LHC §2), to be satisfied on $|\omega| = 1$. The same equation is valid when z is replaced by z_1 and χ by χ_1. But from equation (3.1) we have

$$(\delta + \mathrm{i}\chi_1) = \frac{2\delta}{1+\omega} \tag{4.2}$$

so

$$(\delta + \mathrm{i}\chi_1)\frac{\mathrm{d}}{\mathrm{d}(\mathrm{i}\chi_1)} = -(1+\omega)\frac{\mathrm{d}}{\mathrm{d}\omega}, \tag{4.3}$$

and from (3.2)

$$\frac{\mathrm{d}z}{\mathrm{d}(\mathrm{i}\chi_1)} = (\delta + \mathrm{i}\chi_1)^{-\frac{1}{3}} H(\omega) + \eta(\delta + \mathrm{i}\chi_1)^{\lambda - \frac{4}{3}} \tilde{H}(\omega), \tag{4.4}$$

where

$$H(\omega) = \tfrac{2}{3}B(\omega) - (1+\omega)\,B'(\omega) \tag{4.5}$$

as in LHC §2, while

$$\tilde{H}(\omega) = (\lambda - \tfrac{1}{3})\,\tilde{B}(\omega) - H(\omega)\,\tilde{B}'(\omega). \tag{4.6}$$

Thus from (3.2) and (4.2) we have

$$\left.\begin{aligned} z_1 &= \Delta^2(1+\omega)^{-\frac{2}{3}} B(\omega) + \eta\Delta^{3\lambda-1}(1+\omega)^{-\lambda-\frac{1}{3}}\tilde{B}(\omega), \\ -\mathrm{i}\frac{\mathrm{d}z_1}{\mathrm{d}\chi_1} &= \Delta^{-1}(1+\omega)^{\frac{1}{3}} H(\omega) + \eta^{3\lambda-4}(1+\omega)^{-\lambda-\frac{4}{3}}\tilde{H}(\omega), \end{aligned}\right\} \tag{4.7}$$

and $\Delta = (2\delta)^{\frac{1}{3}}$.

It is convenient to write the boundary condition for z_1 as

$$z_1\frac{\mathrm{d}z_1}{\mathrm{d}\chi_1}\left(\frac{\mathrm{d}z_1}{\mathrm{d}\chi_1}\right)^* + \text{c.c.} = 1, \tag{4.8}$$

where c.c. denotes the complex-conjugate expression. Then on substituting for z_1 and $\mathrm{d}z_1/\mathrm{d}\chi_1$ and considering the terms in η^0 and η^1 respectively we obtain

$$\omega^{-\frac{1}{3}} B(\omega)\,H(\omega)\,H(\omega^{-1}) + \text{c.c.} = 1, \tag{4.9}$$

and

$$\begin{aligned} &(1+\omega)^{1-\lambda}\omega^{-\frac{1}{3}}\tilde{B}(\omega)\,H(\omega)\,H(\omega^{-1}) + \text{c.c.} \\ &+ (1+\omega)^{1-\lambda}\omega^{-\frac{1}{3}} B(\omega)\,\tilde{H}(\omega)\,H(\omega^{-1}) + \text{c.c.} \\ &+ (1+\omega)^{1-\lambda}\omega^{\lambda-\frac{4}{3}} B(\omega)\,H(\omega)\,\tilde{H}(\omega^{-1}) + \text{c.c.} = 0. \end{aligned} \tag{4.10}$$

On extracting the real factor

$$[(1+\omega)(1+\omega^{-1})]^{\frac{1}{2}(1-\lambda)} \tag{4.11}$$

	$\tilde{B}_n$		
n	$N = 30$	N = 40	N = 50
0	0.047765	0.047761	0.047758
1	−0.070711	−0.070706	−0.070702
2	0.014920	0.014921	0.014921
3	0.003529	0.003531	0.003532
4	0.001474	0.001475	0.001476
5	0.000858	0.000858	0.000859
6	0.000570	0.000571	0.000571
7	0.000371	0.000371	0.000372
8	0.000292	0.000292	0.000293
9	0.000192	0.000192	0.000193
10	0.000167	0.000167	0.000167
11	0.000108	0.000108	0.000108
12	0.000101	0.000101	0.000101
13	0.000063	0.000062	0.000062
14	0.000064	0.000064	0.000064
15	0.000037	0.000037	0.000037
16	0.000041	0.000041	0.000041
17	0.000022	0.000022	0.000022
18	0.000028	0.000027	0.000027
19	0.000013	0.000013	0.000013

TABLE 1. Coefficients $\tilde{B}_n$ in the expansion of the modified inner solution, equations (3.2) and (3.4)

from each of the terms in equation (4.10) and writing

$$p = \tfrac{1}{6} - \tfrac{1}{2}\lambda, \quad q = \tfrac{5}{6} - \tfrac{1}{2}\lambda \tag{4.12}$$

we find that (4.10) reduces to

$$\begin{aligned} &H(\omega)\, H(\omega^{-1})\, \omega^p\, \tilde{B}(\omega) + \text{c.c.} \\ &+ B(\omega)\, H(\omega^{-1})\, \omega^p\, \tilde{H}(\omega) + \text{c.c.} \\ &+ B(\omega^{-1})\, H(\omega^{-1})\, \omega^q\, \tilde{H}(\omega) + \text{c.c.} = 0. \end{aligned} \tag{4.13}$$

The functions $B(\omega)$ and $H(\omega)$ are already given in terms of the known coefficients B_n, calculated in LHC, §4. Moreover when $|\omega| = 1$, ω^p may be expanded in the Fourier series

$$\omega^p = \sum_{-\infty}^{\infty} p_n\, \omega^n, \quad \omega = \mathrm{e}^{\mathrm{i}\tau} \tag{4.14}$$

valid in $-\pi < \tau < \pi$, where

$$p_n = \frac{\sin(n-p)\,\pi}{(n-p)\,\pi}. \tag{4.15}$$

Similarly for ω^q. Thus by equating coefficients of $\cos m\tau$, $m = 0, 1, 2, \ldots$, in equation (4.13) we obtain a sequence of linear equations for the unknown coefficients $\tilde{B}_n$. By taking the first $(N-1)$ of these equations and truncating the sequence $\tilde{B}_n$ after $n = N$ we may solve the equations together with (3.9) and (3.10) to find $\tilde{B}_0, \ldots, \tilde{B}_N$. Then N is allowed to increase until the lower coefficients have numerically converged.

The result of this procedure is displayed in table 1, where $\tilde{B}_0, \tilde{B}_1, \ldots, \tilde{B}_{19}$ are given when $N = 30$, 40 and 50. It will be seen that the coefficients have converged effectively to 4 or 5 decimal places.

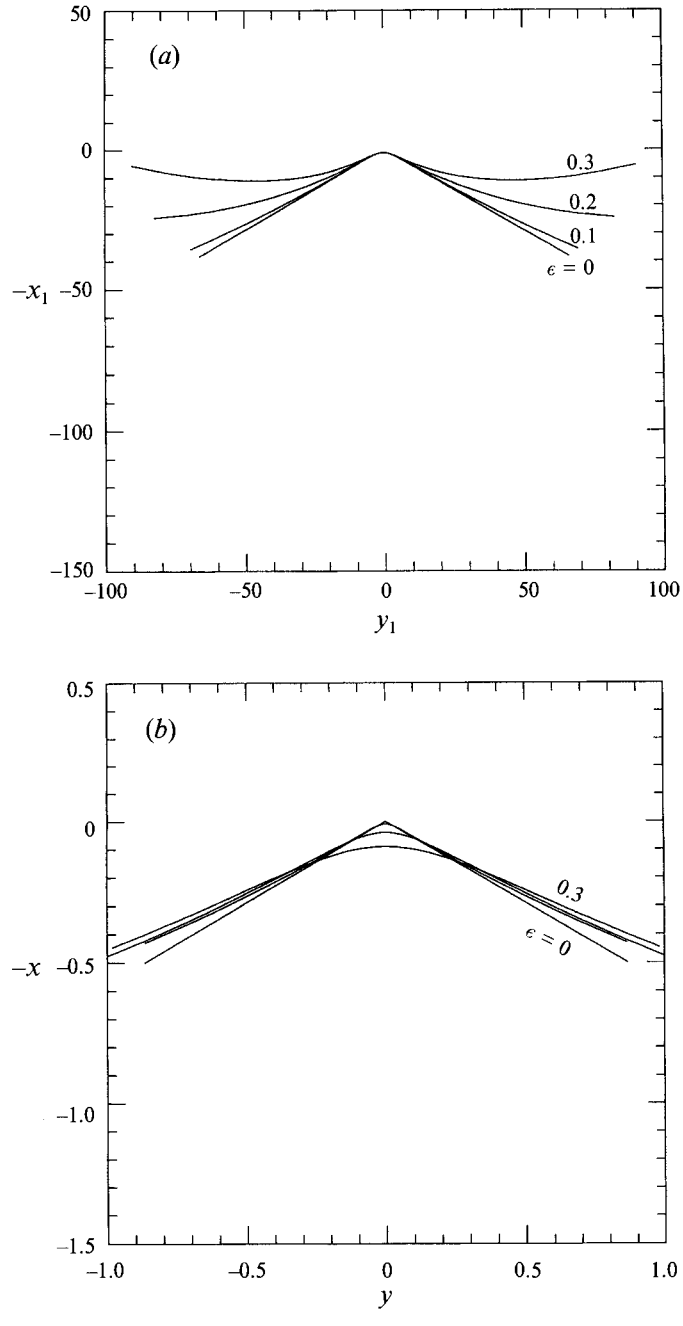

FIGURE 2. Free-surface profiles for the cases $\epsilon = 0$, 0.1, 0.2 and 0.3: (*a*) on the scale of $z_1 = \epsilon^2 z$ and (*b*) on the scale of z.

The corresponding surface profiles are shown in figure 2 for $\epsilon = 0$, 0.1, 0.2 and 0.3. In figure 2(*a*) the profiles are plotted with the scaled coordinate $z_1 = \epsilon^{-2} z$. In figure 2(*b*) they are plotted against z. It should be borne in mind that these represent only the inner solution near the crest of the wave, so that in figure 2(*b*) the region of validity is only within a distance $O(\epsilon^2)$ from the wave crest.

The relation between the parameter ϵ, defined by equation (1.1), and the steepness

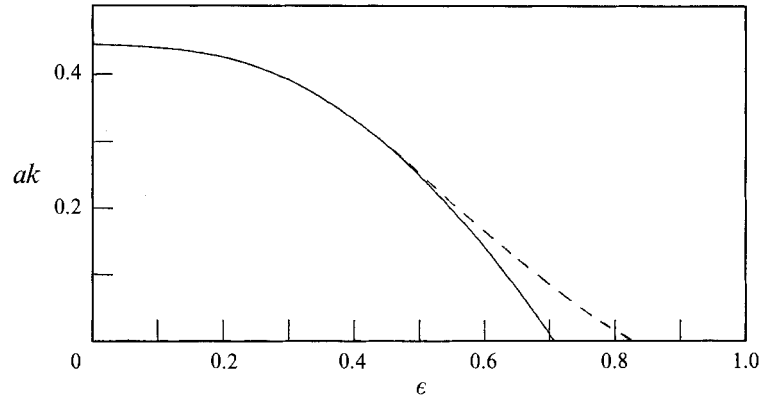

FIGURE 3. Relation between the parameter ϵ and the wave steepness ak. The broken line shows the asymptote (4.16).

parameter ak for progressive irrotational waves in deep water may be calculated directly using Stokes's expansion. The result is shown in figure 3. The dashed line corresponds to the asymptote

$$ak = 0.4432 - 0.50\epsilon^2 + 0.503\epsilon^3 \cos(2.143 \ln \epsilon - 1.54) \tag{4.16}$$

derived in LHF2, equation (5.4).

5. The normal-mode perturbations

To find the normal-mode perturbations of the modified flow we proceed as in §5 of LHC1, that is we write

$$z_1 = Z + \zeta, \tag{5.1}$$

where Z represents the unperturbed, steady flow of equation (3.2) and ζ is a small, time-dependent perturbation whose square we shall neglect. The free surface is specified by

$$\psi_1 = F(\phi_1, t), \tag{5.2}$$

where $\psi_1 = \mathrm{Im}(\chi_1)$ is of the same order as ζ. Then as in LHC1 we are led to the free-surface condition

$$(Z + Z^*) Z_\chi Z_\chi^* = 1 \tag{5.3}$$

at lowest order, and at order ζ

$$\begin{aligned} Z_\chi^*(\zeta_t + \mathrm{i} Z_\chi F_t) = &-\tfrac{1}{2} Z_\chi Z_\chi^* (\zeta + \zeta^*) - \tfrac{1}{2}(Z + Z^*)(Z_\chi^* \zeta_\chi + Z_\chi \zeta_\chi^*) \\ &+ \tfrac{1}{2}\mathrm{i}\,[(Z + Z^*)(Z_\chi Z_{\chi\chi}^* - Z_\chi^* Z_{\chi\chi}) + (Z_\chi^* - Z_\chi) Z_\chi Z_\chi^*] F \\ &- \mathrm{i} F_{\phi_1}, \end{aligned} \tag{5.4}$$

both to be satisfied on $\psi_1 = 0$.

Now from (3.2) and (4.2) we have

$$Z = \left(\frac{2\delta}{1+\omega}\right)^{\frac{2}{3}} B(\omega) + \eta \left(\frac{2\delta}{1+\omega}\right)^{\lambda - \frac{1}{3}} \tilde{B}(\omega), \tag{5.5}$$

that is

$$Z = \Delta^2 (1+\omega)^{-\frac{2}{3}} \tilde{\tilde{B}}(\omega), \tag{5.6}$$

where $\Delta = (2\delta)^{\frac{1}{3}}$ and

$$\tilde{\tilde{B}}(\omega) = B(\omega) + \eta \Delta^{3(\lambda-1)} (1+\omega)^{1-\lambda} \tilde{B}(\omega), \tag{5.7}$$

a known function, expansible in positive powers of ω. From (5.6) we may also write

$$\left.\begin{aligned} Z_\chi &= \mathrm{i}\Delta^{-1}(1+\omega)^{\frac{1}{3}}\tilde{\tilde{H}}(\omega), \\ Z_{\chi\chi} &= \Delta^{-4}(1+\omega)^{\frac{4}{3}}\tilde{\tilde{G}}(\omega), \end{aligned}\right\} \tag{5.8}$$

where

$$\left.\begin{aligned} \tilde{\tilde{H}}(\omega) &= \tfrac{2}{3}\tilde{\tilde{B}}(\omega)-(1+\omega)\,\tilde{\tilde{B}}'(\omega), \\ \tilde{\tilde{G}}(\omega) &= \tfrac{2}{9}\tilde{\tilde{B}}(\omega)-\tfrac{2}{3}(1+\omega)\,\tilde{\tilde{B}}'(\omega)-(1+\omega)^2\tilde{\tilde{B}}''(\omega), \end{aligned}\right\} \tag{5.9}$$

and a prime denotes $\mathrm{d}/\mathrm{d}\omega$. Similarly if

$$\zeta = C(\omega) \tag{5.10}$$

then

$$\zeta_\chi = -\mathrm{i}\Delta^{-3}(1+\omega)\,E(\omega), \tag{5.11}$$

where

$$E(\omega) = (1+\omega)\,C'(\omega). \tag{5.12}$$

then on substituting in equation (5.4) we obtain

$$-\mathrm{i}\frac{\partial}{\partial t}[P(\omega)\,C(\omega)-R(\omega)\,F(t)] = \mathrm{Re}\,[Q(\omega)\,E(\omega)-R(\omega)\,C(\omega)]$$

$$+2\mathrm{i}\left[(1+\cos\tau)\frac{\mathrm{d}F}{\mathrm{d}\tau}+S(\omega)\,F(\tau)\right] \tag{5.13}$$

to be satisfied on

$$\omega = \mathrm{e}^{\mathrm{i}\tau}, \quad -\pi < \tau < \pi. \tag{5.14}$$

In equation (5.14), P, Q, R, S are precisely the same functionals of $\tilde{\tilde{B}}$, $\tilde{\tilde{H}}$ and $\tilde{\tilde{G}}$ as they are of B, H and G in equation (5.16) of LHC1. Moreover, since $\tilde{\tilde{B}}(\omega)$, like $B(\omega)$, is expansible in positive powers of ω, all the remainder of §5 of LHC1 applies also. Thus we may seek normal-mode solutions in which ζ and F have a time dependence like $\mathrm{e}^{\beta t}$, and proceed to determine β in a similar manner.

6. Results

Calculations of the eigenvalues were carried out with $\delta = 10^{\frac{3}{2}}$ as in LHC1 and ϵ in the range 0 to 0.105. It was found that all the eigenvalues β^2 were real. Moreover, only the lowest eigenvalue β_0^2 was positive, corresponding to an exponential growth or decay rate β_0. In figure 4 β_0^2 is plotted as a function of ϵ, and will be seen to be a steadily decreasing function of ϵ, diminishing from $\beta_0^2 = 0.00292$ at $\epsilon = 0$ to zero at about $\epsilon = 0.102$, apparently. The computation is valid, however, only for sufficiently small values of ϵ.

It is more revealing to consider the unscaled growth rate $\beta/\sigma\epsilon$, relative to the radian frequency σ of a progressive deep-water wave of low amplitude ($\sigma^2 = gk$, where k is the wavenumber). Figure 5 shows $(\beta_0/\epsilon\sigma)^2$ plotted against the wave steepness ak. The curve on the upper right of the diagram corresponds to that in figure 4, the same portions being shown by solid or broken curves. The remaining plots in figure 5 are of the frequencies of the lowest (non-trivial) superharmonic mode of a progressive wave of finite amplitude, as calculated by Tanaka (1983) and Longuet-Higgins (1978, 1986). The quantity $-\sigma_2^2/\sigma^2$ is plotted from figure 7 of Tanaka (1983) and table 2(*b*) of Longuet-Higgins (1986). These calculations demonstrated that the lowest mode becomes unstable at around $ak = 0.4292$, where the energy density has a local maximum (see also Saffman 1985). This point is marked by a cross ($\times$) in figures 4 and 5.

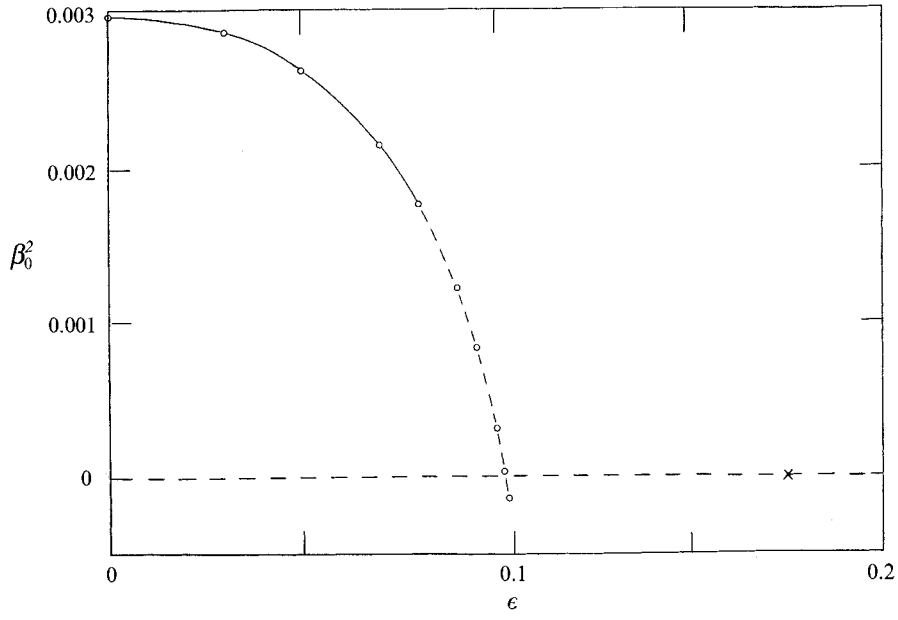

FIGURE 4. The rate of growth β_0 of the unstable mode. β_0^2 is shown as a function of ϵ.

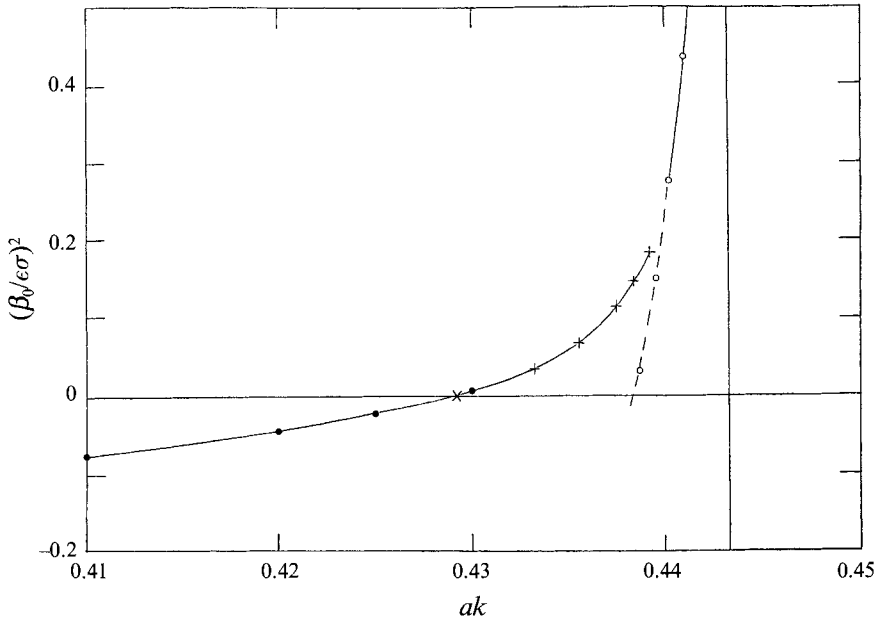

FIGURE 5. Growth rates of the crest instability compared with those of the lowest superharmonic instability in a progressive, irrotational wave in deep water: O——O $(\beta_0/\sigma)^2$, from figure 4; ●——● $-(\sigma_2/\sigma)^2$ from Longuet-Higgins (1978, 1986); +---+ $-(\sigma_2/\sigma)^2$ from Tanaka (1983).

From figure 5 it appears that the calculations of the present paper provide an asymptote for the previous calculations of the lowest superharmonic instability, in the limit as $\epsilon \to 0$ and $ak \to (ak)_{\max}$. In other words, the superharmonic instability is associated primarily with the instability of the flow near the wave crest; it is a 'crest instability'.

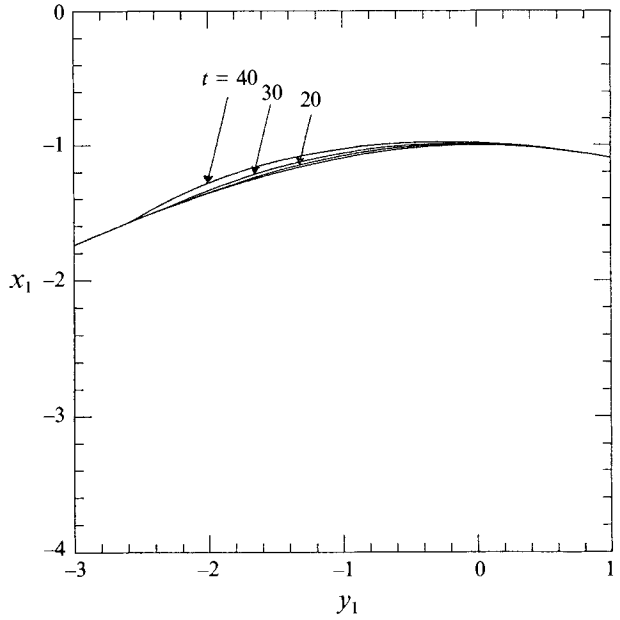

FIGURE 6. Form of the free-surface profile in the growing instability, when $\epsilon = 0.08$.

Secondly, the asymptotic analysis, so far as it has been carried in the present paper, is valid only for sufficiently small values of ϵ (as one would expect). Figure 5 suggests that the limit of validity is at about $\epsilon = 0.08$ ($ak = 0.440$). More accurate calculations of this instability from the present point of view would have to take account of the flow not only in the inner zone I (see §2 above) but also in the matching zone II and hence also the flow in zone III. This would imply corrections depending upon higher powers of ϵ.

The displacement of the free surface corresponding to the growing unstable mode is shown in figure 6, for the case $\epsilon = 0.08$. It will be seen to be practically identical in form to the case $\epsilon = 0$, shown in figures 3 and 4 of LHC. That is, the fluid near the crest is displaced forwards, and the 'toe' of the breaker occurs at about $y_1 = -2.3$. The chief discernible difference is in the rate of growth β_0, which is 0.0544 when $\epsilon = 0$ and 0.0421 when $\epsilon = 0.08$. According to figure 4, β_0^2 decreases almost parabolically with ϵ, so that

$$\beta_0^2 = 0.00296 - 0.030\epsilon^2. \tag{6.1}$$

Hence in the unscaled time frame the rate of growth $\beta' = \beta_0/\epsilon\sigma$ relative to the radian frequency σ of a progressive wave in deep water (and of small slope) may be written

$$\beta' = 0.0544\epsilon^{-1}(1 - 0.05\epsilon^2), \tag{6.2}$$

generalizing equation (6.5) of LHC. This is valid only when $0 \leqslant \epsilon \leqslant 0.08$. Since over this range $\epsilon^2 \approx 2\Delta ak$, where Δak is the difference between the steepness parameter ak and its limiting value 0.4432, we have also

$$\beta' \approx 0.0385(\Delta ak)^{-\frac{1}{2}}(1 - 0.10\Delta ak) \tag{6.3}$$

over the same range.

Tanaka (1983) does not describe the surface profile of the instability in his calculations, so that changes in the form of the instability in the range $0.4292 < ak < 0.44$ cannot be ruled out.

7. Conclusions and discussion

We have extended the stability calculations for the almost-highest wave to waves of slightly lower steepness ak, taking into account the lowest-order perturbation to the inner flow, which is of order $\epsilon^{3(\lambda-1)}$. As before, there is just one unstable mode for the inner flow, with a form resembling the initial stages of a spilling breaker. Its rate of growth β_0 is a decreasing function of the perturbation parameter ϵ. The curve of β_0/ϵ as a function of the wave steepness parameter ak is found to be a satisfactory asymptote to Tanaka's previously calculated values of the lowest superharmonic instability ($n = 2$). The form of the instability is almost independent of ϵ and k when $0 \leqslant \epsilon \leqslant 0.08$, but the rate of growth depends strongly on ϵ.

The lowest superharmonic instability becomes unstable at the lowest value of ak for which the wave energy density is a maximum ($ak = 0.4292$). As mentioned by Tanaka (1985, §4) the next highest superharmonic mode ($n = 3$) becomes unstable also, but at the next highest stationary value of the energy, as a function of ak. We may conjecture that this mode also tends asymptotically to a form described by the theory of the almost-highest wave.

From these results we have drawn the conclusion that the reason for the existence of the superharmonic instability is the form of the flow in the crest of the wave; it is essentially a 'crest instability'. The fact that the superharmonic mode first becomes unstable at a stationary value of the energy in the wave as a whole need not deter us from this conclusion. For the maximum of the energy can itself be regarded as a result of the peculiar form of the flow in the almost-highest wave, as described by the inner flow near the wave crest.

The form of the inner flow described in LHC1 is not of course limit to steep, periodic waves in deep water; it will apply also to periodic waves in water of finite depth, or to solitary waves in shallow water, for example. However the modification to the inner flow, which depends on the nature of the outer flow, will be different in the various cases. From our results for deep water, it seems likely that this modification to the inner flow will affect the rate of growth, but not the form, of the crest instability.

Finally, it is possible that similar conclusions will apply to the final breaking of waves that are not strictly periodic, such as those associated with wave groups which arise from *sub*harmonic instabilities of the Benjamin–Feir type; see Longuet-Higgins & Cokelet (1978), Dold & Peregrine (1987). Such numerical calculations certainly suggest that the ultimate overturning of the crest of a gravity wave has a characteristic form, largely independent of its previous history of growth.

In mixed seas, having a broad frequency spectrum, the situation is different. There, the field observations by Holthuijsen & Herbers (1986) show that breaking can occur at much lower wave steepnesses; $ak = 0.3$ is a typical value. Such breaking is probably initiated by a more global type of instability, leading to strong fore-and-aft asymmetry of the waves prior to overturning. The process of formation of the final jet, however, may have some features in common with the much smaller jet arising from a crest instability.

The implications for very short gravity waves should also be recalled from LHC. There it was pointed out that as soon as the crest instability grows sufficiently to induce a sharp curvature on the forward shape of the wave, surface tension may intervene to produce parasitic capillary waves ahead of the sharp curvature, as is often observed. There may also be a 'capillary roller' following the sharp curvature, which will lead to the roughness and ultimate crumpling of the wave crest – a quite distinct style of wave breaking; see Longuet-Higgins (1993).

The present paper is based in part on Chapter 7 of Fox (1977) and chapter 8 of Cleaver (1981). The calculations have been completely reworked and extended by M.S.L.-H. This study has been supported by the Office of Naval Research under Contract N00014-91-J-1582.

REFERENCES

CLEAVER, R. P. 1981 Instabilities of surface gravity waves. PhD thesis, University of Cambridge.

DOLD, J. W. & PEREGRINE, D. H. 1987 Water-wave modulation. In *Proc. 20th Intl Conf. on Coastal Engng, Taipeh, Nov.* 1986, pp. 163–175. ASCE.

FOX, M. J. H. 1977 Nonlinear effects in surface gravity waves. PhD. thesis, University of Cambridge.

GRANT, M. A. 1973 The singularity at the crest of a finite amplitude Stokes wave. *J. Fluid Mech.* **59**, 257–262.

HOLTHUIJSEN, L. H. & HERBERS, T. H. C. 1986 Statistics of breaking waves observed as white-caps in the open sea. *J. Phys. Oceanogr.* **16**, 290–297.

LONGUET-HIGGINS, M. S. 1986 Bifurcation and instability in gravity waves. *Proc. R. Soc. Lond.* A **403**, 167–187.

LONGUET-HIGGINS, M. S. 1993 The crest instability of steep gravity waves *or* How do short waves break? *Proc. Air–Sea Interface Symp. June 1993, Marseille, France* (ed. M. A. Donelan) (to appear).

LONGUET-HIGGINS, M. S. & CLEAVER, R. P. 1994 Crest instabilities of gravity waves. Part 1. The almost-highest wave. *J. Fluid Mech.* **258**, 115–129 (referred to herein as LHC).

LONGUET-HIGGINS, M. S. & COKELET, E. D. 1978 The deformation of steep surface waves on water. II. Growth of normal-mode instabilities. *Proc. R. Soc. Lond.* A **364**, 1–38.

LONGUET-HIGGINS, M. S. & FOX, M. J. H. 1977 Theory of the almost-highest wave: the inner solution. *J. Fluid Mech.* **80**, 721–741 (referred to herein as LHF1).

LONGUET-HIGGINS, M. S. & FOX, M. J. H. 1978 Theory of the almost-highest wave. Part 2. Matching and analytic extension. *J. Fluid Mech.* **85**, 769–786 (referred to herein as LHF2).

SAFFMAN, P. G. 1985 The superharmonic instability of finite amplitude water waves. *J. Fluid Mech.* **159**, 169–174.

TANAKA, M. 1983 The stability of steep gravity waves. *J. Phys. Soc. Japan* **52**, 3047–3055.

TANAKA, M. 1985 The stability of steep gravity waves. Part 2. *J. Fluid Mech.* **156**, 281–289.